9-18-2012

Sequential ionization and energy gain of bound electrons in classical modeling of atoms in strong laser fields

Stanley L. Haan
Calvin University

K. N. Shomsky
Calvin University

N. A. Danks

Sequential ionization and energy gain of bound electrons in classical modeling of atoms in strong laser fields

S. L. Haan,* N. A. Danks, and K. N. Shomsky
Department of Physics and Astronomy, Calvin College, Grand Rapids, Michigan 49546, USA
(Received 28 January 2012; published 18 September 2012)

Classical mechanics and classical ensembles have provided numerous insights into the dynamics of strong-field double ionization. In this paper, we show that in classical multidimensional modeling, the laser intensity at which sequential ionization begins to dominate depends on the softening of the interaction between the electron and nucleus. We show that an unsoftened interaction in two or three dimensions can lead to classical orbits in which an electron can start deep in the nuclear potential-energy well, gain energy from the oscillating laser field, and ionize over the barrier without any recollision. We discuss how this energy gain occurs, with the electron orbit favoring one side of the nucleus or the other, depending on which side corresponds with the rising potential-energy curve.

DOI: 10.1103/PhysRevA.86.033418 PACS number(s): 32.80.Rm, 32.60.+i

I. INTRODUCTION

Multielectron atoms in strong laser fields are remarkably complex nonlinear systems that have proven challenging to understand [1]. Theoretical investigations of such systems have employed various approaches, including quantum-mechanical *S*-matrix [2] and numerical studies, semiclassical [3] models, and fully classical analyses. Two electrons in three dimensions have six degrees of freedom, posing huge computational challenges for fully quantum-mechanical studies [4]. Consequently, most of the quantum-mechanical studies have restricted the electrons to one dimension [5] with a soft-core potential [6]. These quantum studies for two-electron systems revealed very classical behavior [7] and helped to stimulate fully classical examinations [8]. These are effective (especially at visible and infrared wavelengths) because of the very strong oscillating field and the quantum-mechanical state mixing that it induces. Classical studies are easily generalizable to two electrons in three dimensions (see, e.g., [9] and [10]) and have helped to provide valuable insight into the dynamics of nonsequential double ionization. Classical studies are also generalizable to three electrons in multiple dimensions [11] and to molecular systems [12].

It is important to understand the characteristics and behavior of classical ensembles because such ensembles may be widely used in coming years for investigating complex systems in external fields. Ensembles also link strong-field atomic physics with the fields of nonlinear dynamics and chaos [13].

In fully classical systems, all escapes are over the barrier—there is no tunneling. For a two-electron system, the first ionization can occur in part through energy sharing by the two electrons. One electron escapes over a suppressed barrier when the laser field is strong, leaving the other fairly deep in the well. In the usual three-step model of nonsequential double ionization [3], the inner electron remains deep in the well until the other electron returns and imparts energy through recollision. The inner electron may be directly ionized by the collision, or there may be recollision excitation with subsequent ionization. An alternative to recollision is independent sequential ionization, usually just called sequential ionization, in which the inner electron escapes the well without the benefit of additional energy from recollision. The primary question we consider in the present paper regards the ability of the inner electron to ionize without any recollision. In a quantum-mechanical system, we might say that this electron could absorb photons or tunnel through the barrier to escape. But what about in a classical system? Mauger *et al*. [13] have shown that in one-dimensional (1D) systems, there is a stable inner region of phase space from which an electron does not escape, and a higher energy region from which it may escape if given sufficient time. In the present paper, we consider an electron in a potential-energy well that is exposed to an oscillating laser field, and we examine the electron's ability to absorb energy from the laser and thereby escape the well.

II. SEQUENTIAL IONIZATION IN 3D CLASSICAL ENSEMBLES

One characteristic of classical atoms is the possibility for autoionization—if there is no lower bound on a confined electron's energy, then *e*-*e* energy sharing can allow one electron to dive deep into the well while the other escapes. This challenge can be met by softening the interaction with the nucleus [14] and thereby introducing a minimum value for the potential energy. In our ensemble work, we typically have replaced the Coulomb potential $-2/r$ with the softened potential $-2/\sqrt{r^2+a^2}$, with $a = 0.825$ a.u. (We use atomic units unless otherwise specified.) Then the minimum value for the potential is $-2/a = -2.42$, which is somewhat below the energy -2 of the actual helium ion. Two electrons with combined energy equal to the helium ground state (-2.24) can jostle and share energy without either one being able to escape the nuclear well until the laser is turned on.

In Ref. [15], Haan and Smith noted that if one electron ionizes and then returns to the nucleus, then it can backscatter only if it encounters a strong force from the nucleus—and a softened potential will not allow for backscattering. Consequently, they adopted a rather *ad hoc* approach of changing the softening parameter, trajectory by trajectory, after the first ionization. We do the same—after one electron ionizes, we change the value of the softening parameter from 0.825 to either 0.01 or 0.4. We adjust the softening for both

*haan@calvin.edu; http://www.calvin.edu/~haan

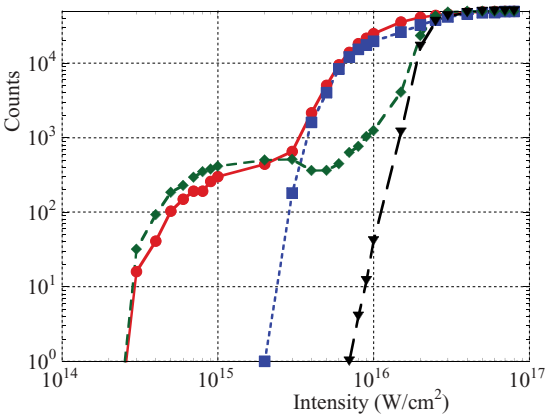

FIG. 1. (Color online) Double-ionization yield vs laser intensity for three-dimensional classical ensembles, with different values of the nuclear softening parameter a after the first ionization (as described in the text). For $a = 0.4$, the green dashed curve with diamonds is the total DI yield and the black long-dashed curve with inverted triangles is the sequential yield. For $a = 0.01$, the red solid curve with circles is the total DI yield and the blue dotted curve with squares is the sequential yield. The onset for sequential ionization occurs at a lower intensity for a more exposed nucleus. Laser wavelength $\lambda = 800$ nm, ensemble size 50 000 atoms, with a trapezoidal $(1 + 3 + 1)$ pulse.

electrons simultaneously, and we account for any decrease in potential energy with a compensatory change in (radial) kinetic energy, so total energy remains fixed. One good feature of this approach is that it allows for exploration of the importance of the details of the interaction between the electrons and nucleus.

In Fig. 1, we show the double-ionization (DI) yield vs laser intensity for wavelength 800 nm and for the two different values of the final softening parameter, 0.01 and 0.4. In both cases, we obtain the familiar knee or plateau, but the plateau applies over a much shorter intensity range for the less softened potential [16].

We have backtracked all DI trajectories and classified them according to their ionization mechanism. In sequential ionization [17], the second electron escapes the well without absorbing energy from the first electron (i.e., without recollision). The figure shows sequential-ionization yields for each case and indicates that the transition to sequential ionization occurs at a lower intensity for the less softened potential.

If one checks the initial energies and the amount of barrier suppression, it immediately becomes evident that the sequential ionization of Fig. 1 occurs because the electron that is left behind in the core is able to absorb energy from the laser and "climb out" of the well. Our results suggest that the escape dynamics may be different in the multidimensional case than in the one-dimensional cases previously studied (e.g., in [13]).

III. ELECTRON ENERGY ABSORPTION IN TWO DIMENSIONS

To investigate why sequential ionization "turns on" at different intensities for the two different softening parameters, we focus our attention on the simpler case of one electron in a 2D well exposed to an oscillating linearly polarized laser field. We will return to our 3D, two-electron ensemble after

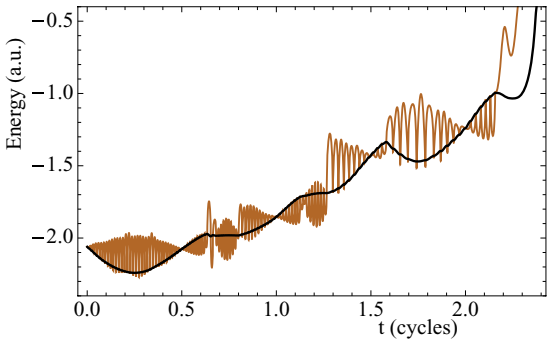

FIG. 2. (Color online) Electron energy vs time for a single electron with an oscillating laser field in a 2D nuclear well, with nuclear softening parameter $a = 0.01$. The electron absorbs energy and escapes the well. The oscillatory curve (brown) neglects the laser interaction energy $+zE_0\sin(\omega t)$, whereas the smoother curve (black) includes it.

we analyze this simpler system. We write the energy as

$$E = \frac{v^2}{2} - \frac{2}{\sqrt{x^2 + z^2 + a^2}} + zE_0\sin\omega t, \qquad (1)$$

where v is the speed, x and z are position coordinates, a is the softening parameter, E_0 is the laser electric-field amplitude, and ω is the laser angular frequency. We set $a = 0.01$, $E_0 = 0.293$ (intensity 3×10^{15} W/cm^2), and $\omega = 0.0570$ a.u. (wavelength 800 nm).

A. An example trajectory

Figure 2 shows energy vs time for one ionizing trajectory for this system. The figure clearly shows the ability of the classical electron to absorb energy and escape the well. The (dark) smoother curve shows the energy as defined in Eq. (1), whereas the (light) oscillating curve excludes the laser interaction energy, $+zE_0\sin\omega t$. For the latter curve, the laser is external to the system, and each oscillation in the well becomes evident as the laser force alternately does positive or negative work on the electron. The electron's oscillations in the well occur on much shorter time scales than the laser cycle. The two curves cross whenever $z = 0$ and at each half cycle when the laser field goes through zero.

We now focus our attention on the shorter time scale from $t = 1.0$ to 1.5 cycles, an interval in which there is significant energy gain. In Fig. 3, we show energy vs time and the z coordinate vs time for this interval, as well as the spatial trajectory over a short interval around the field maximum at 1.25 cycles. We show cross sections of the 2D potential-energy well at specific times in Fig. 4. There the dashed horizontal line segment shows the energy of maximum barrier suppression.

From Fig. 3, we learn that for this time interval, the electron's orbit is primarily on the $z > 0$ side of the nucleus until about time 1.27 cycles, then switches to being primarily on the $z < 0$ side of the nucleus. It is this switch and its timing at about the laser maximum of 1.25 cycles that leads to the energy gain, as we explain more fully below.

When the laser interaction energy $+zE_0\sin\omega t$ is included in the electron energy, the electron can gain or lose energy depending on its z coordinate as the laser field strength

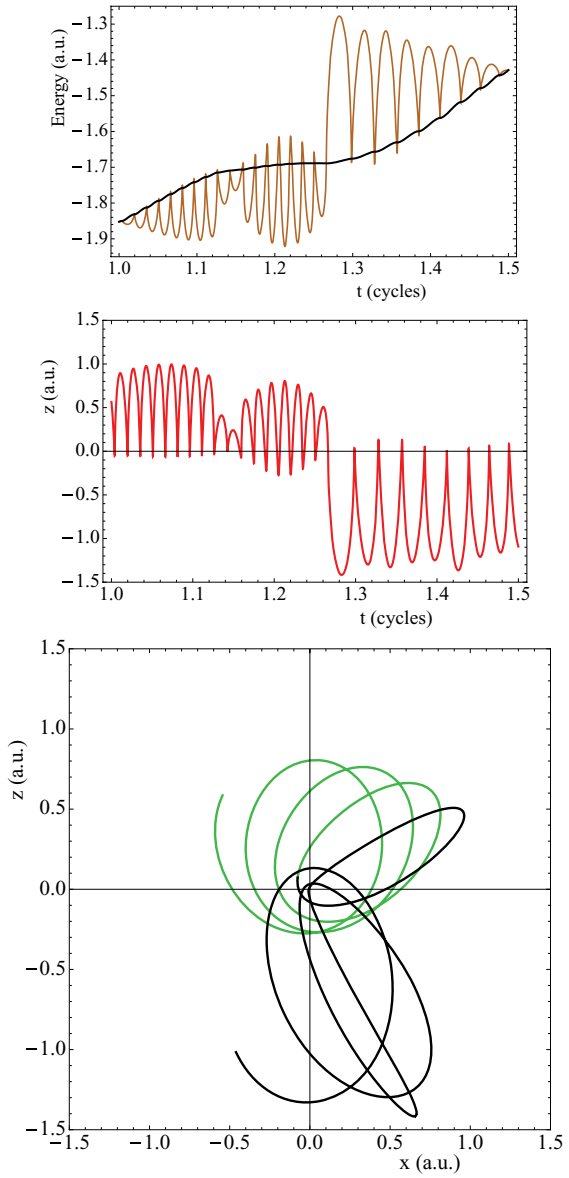

FIG. 3. (Color online) Top: Electron energy vs time, with (black smooth curve) and without (brown oscillatory curve) the laser interaction, for the trajectory of Fig. 2, zoomed in on $1.0 < t < 1.5$ cycles. Center: z coordinate of that same electron. The curves in the top plot cross whenever $z = 0$. Bottom: Spatial trajectory for a few oscillations before and after $t = 1.25$ cycles. The curve changes from green to black (light to dark) at $t = 1.25$ cycles (second quadrant, close to the origin). The electron switches its oscillation from one side of the nucleus to the other at about 1.27 cycles, when the laser force is strong in the $-z$ direction. That switch plays a key role in the electron's energy increase.

changes. It can "ride" an increasing laser potential to greater energy or a decreasing laser potential to lower energy. The electron of Fig. 3 is primarily on the $z > 0$ side of the nucleus during the interval from $t = 1.0$ to 1.25 cycles; during this time, the $z > 0$ side of the potential energy curve is rising (see Fig. 4) and, consequently, the electron's energy increases. After $t = 1.25$ cycles, the $z > 0$ side of the curve begins to drop back down, and the $z < 0$ side begins to rise. If the electron had maintained an orbit primarily on the $z > 0$ side of the nucleus, it could have lost the energy it had gained during the previous quarter cycle, but instead it jumps to an orbit that favors the $z < 0$ side of the nucleus (or perhaps we should say the electron is pushed to that side by the laser), and the electron continues to gain energy by "riding" the rising side of the potential-energy curve.

The ability to have a net energy absorption thus seems to be related to having an orbit that favors a specific side of the nucleus during specific half cycles. Such orbits can arise when there is low angular momentum and an unshielded nucleus—the electron can come close to the nucleus and experience the large force needed for an abrupt change in the direction of motion. By contrast, a softened nuclear potential is flat near $r = 0$ and does not provide sufficiently large force for the abrupt direction change.

If the electron's orbit did not jump from favoring one side of the nucleus to the other, then it could alternately gain and lose energy. This is evident, for example, in Fig. 2 from $t = 0$ to 0.5 cycles. For the entire half cycle from $t = 0$ to 0.5 cycles, the electron is primarily on the side of the nucleus toward which the laser is pushing ($z < 0$). However, during the next half cycle, the laser pushes in the opposite direction, and the electron's orbit changes so that by the end of that half cycle, the electron is again favoring the side of the nucleus toward which the laser pushes. The result is a net increase in energy. The "jump" from an orbit primarily favoring one side of the nucleus to an orbit favoring the other side is not completely random, but due in part to the force from the laser.

The angular momentum L ($=L_y$) vs time is shown in Fig. 5, along with the x and z position coordinates. The angular momentum changes sign very shortly after the jump. In examining other trajectories, we have noted that orbital jumps are very frequently associated with zeros or minima in $|L|$, and, consequently, angular momentum is worthy of further consideration. A jump from an orbit favoring the $z > 0$ side of the nucleus to one favoring the $z < 0$ side (or vice versa) can be achieved if the electron travels nearly radially in the $\pm z$ direction—and radial motion is precisely the condition for a minimum or a zero in L. Changes in L can only arise from the torque from the laser force, and since the laser force is always in the $\pm z$ direction, the torque in our 2D system depends on the x coordinate of the particle's position. The orbital spiral for our example trajectory has several spirals that favor $x > 0$ and a torque in the $+y$ direction. Thus, L increases from roughly -0.8 toward zero (we maintain a right-handed coordinate system, so the $+y$ direction is into the page). The jump occurs when the electron penetrates very close to the nucleus and scatters into the $-z$ direction, thus illustrating how jumps can correlate with zeros or minima in $|L|$. In the example trajectory of Figs. 3–5, the electron continues to oscillate primarily on the $x > 0$ side of the nucleus after the jump, so L continues to grow more positive. If the electron's initial turning point after the jump had $x < 0$, then the torque would have been negative and the angular momentum would have returned to a negative value. We have examined numerous other trajectories, and found that the orbital jumps from one side of the nucleus to the other can be associated with minima in $|L|$, but there need not be a sign change for L.

An alternative description of the energy gain can be given if one wishes to treat the laser as external to the system, as in

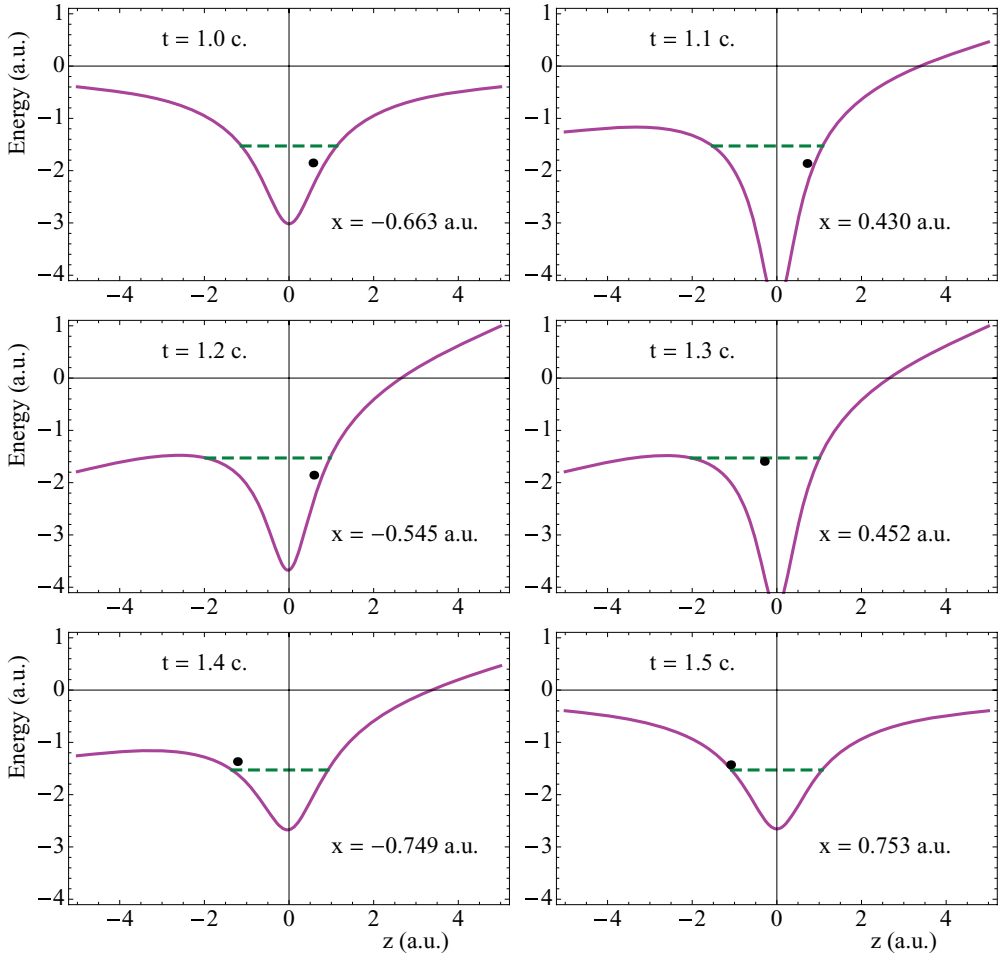

FIG. 4. (Color online) Effective energy plots from $t = 1.0$ through 1.5 cycles for the same trajectory as the previous figure. The dashed horizontal line segment shows the lowest barrier height. The electron gains or loses energy depending on its value of z as the laser raises the potential-energy curve on one side of the nucleus and reduces it on the other side. We plot the potential energy vs z for the actual x value of the electron; the parametric dependence on x changes the shape of the well [18].

the highly oscillatory curves of electron energy. Then the laser alternates between doing positive and negative work with each half orbit of the electron. Slight variations in work done from one half cycle to the next can accumulate. Critically, if the electron orbit changes from favoring one side of the nucleus to favoring the other, then as the orbit changes, the electron can have an extended path in the direction of the laser force and considerable positive work can be done. The corresponding big jumps in energy are clearly evident in the figures.

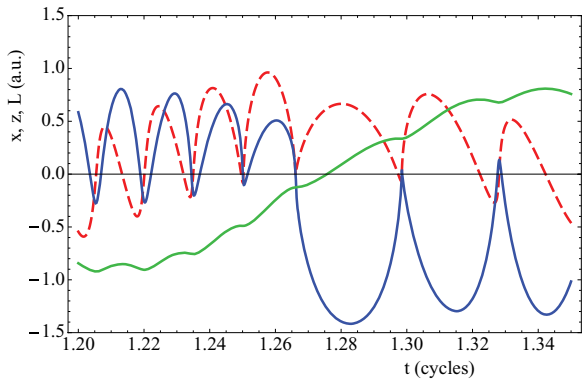

FIG. 5. (Color online) Position coordinates x (dashed red or light curve) and z (solid blue or dark curve) vs time, as well as angular momentum L (solid green curve, transitioning from $-$ to $+$) vs time. The angular momentum of the orbit increases as the "jump" to the new orbit approaches, then passes through zero just after the jump.

B. 1D and 2D ensemble behavior and dependence on softening parameter

To investigate the universality of an electron's ability to absorb energy and escape from a well, we have done systematic variations of the initial conditions for classical electrons in one and two dimensions, and with different values of the softening parameter. In each case, we exposed the electron to an electric force, $-E_0 \sin\omega t$, and then calculated the electron energy (excluding the laser interaction) 2.75 cycles later. We consider the final energy at a time of peak laser field because if no forces other than the laser were acting, then the energy at the peak field would correspond to the electron's drift energy. The results are shown in Fig. 6. On the left, we show results for

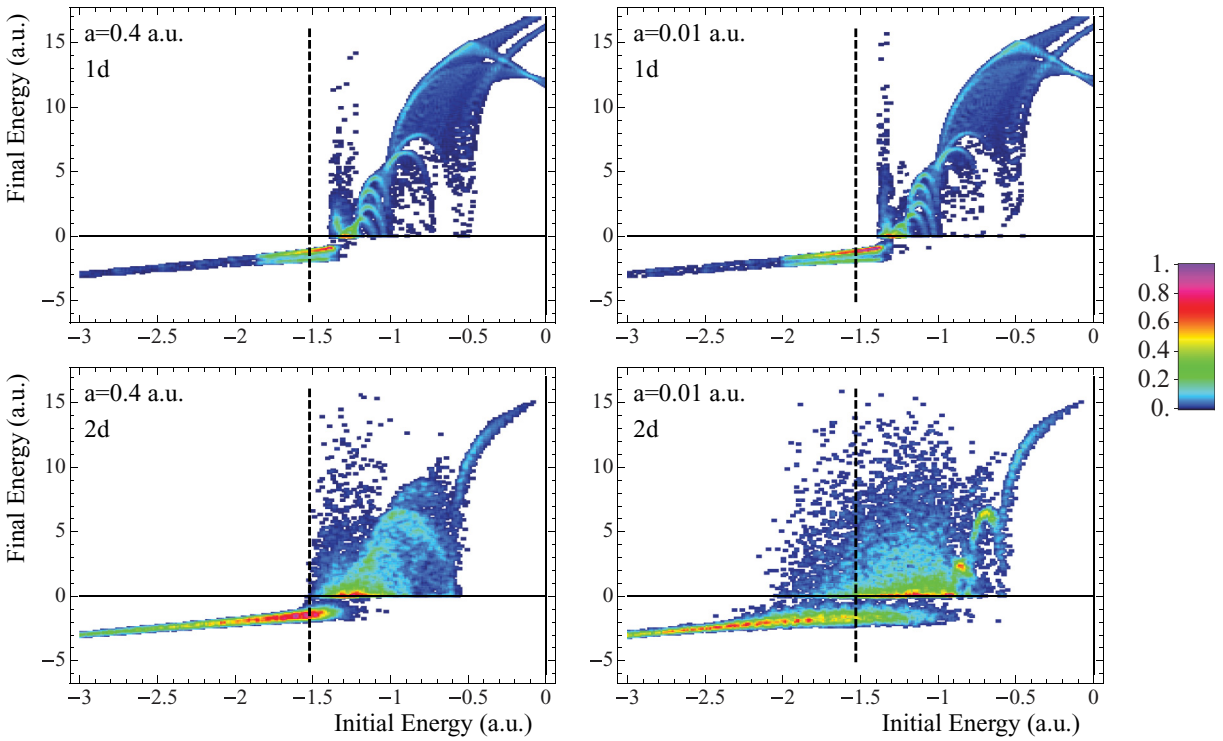

FIG. 6. (Color online) Electron energy (excluding the laser interaction) at $t = 2.75$ cycles vs electron energy at $t = 0$ cycles for a single electron in a nuclear potential-energy well exposed to a sinusoidal laser force at $I = 3 \times 10^{15}$ W/cm^2 with $\lambda = 800$ nm. The nuclear potential energy is $-2/\sqrt{r^2 + a^2}$. In all plots, the vertical dashed line shows the energy of the maximally suppressed barrier. Top left panel: 1D, $a = 0.4$. Top right panel: 1D, $a = 0.01$. Bottom left panel: 2D, $a = 0.4$. Bottom right panel: 2D, $a = 0.01$. For all plots, the initial positions and velocities were systematically varied. The electron can "climb" out of the well only for the unsoftened potential in multiple dimensions.

a softened nucleus, $a = 0.4$, and on the right, we show results for a less softened nucleus, $a = 0.01$. The top row applies for a one-dimensional system, and the bottom row applies for a two-dimensional system. In each image, the vertical dashed line identifies the energy of the maximally suppressed barrier (i.e., the saddle-point energy at peak field, and the minimum energy needed for a classical particle to escape the well). In one dimension, electrons must start with energy greater than this reference energy in order to escape. For the two-dimensional system, results depend on the softening parameter. For $a = 0.4$ (bottom left), the vertical bar closely matches the threshold initial energy for escape. In contrast, at $a = 0.01$ (bottom right), electrons are able to start with energy significantly below the barrier energy and still escape the nuclear well. This establishes the key result that for the unsoftened nuclear potential in multiple dimensions, the electron can absorb energy and climb out of the nuclear potential well, but for other cases remains trapped. For completeness, we comment that for the 2D case, the initial conditions were systematically varied from $0.2 < x_0 < 1.4$, $-1.4 < z_0 < -0.2$, $0 < v_{0x} < 1$, and $-1 < v_{0z} < 0$, each with a step size of 0.1.

Final energies can reach about 15 a.u. or 2.4 U_p. These high energies can be achieved through what Ref. [15] dubbed a boomerang—the laser force pushes a bound electron outward from the nucleus in one direction, but the electron remains bound and the oscillating laser force goes to zero at about the same time as the nucleus stops the outward motion. The nucleus and laser then act together in the opposite direction; the electron traverses the region of the nucleus and reaches the other side of the well just as the laser suppresses the barrier, allowing escape and the possibility of final energy above $2U_p$. This mechanism was discussed in [19] as an important post-recollision ionization mechanism leading to high-energy electrons.

We comment that calculating the energy at the peak field as we have done may give slightly different results from calculating the final energy after ramping the field amplitude to zero. For example, in the latter case, there is the possibility

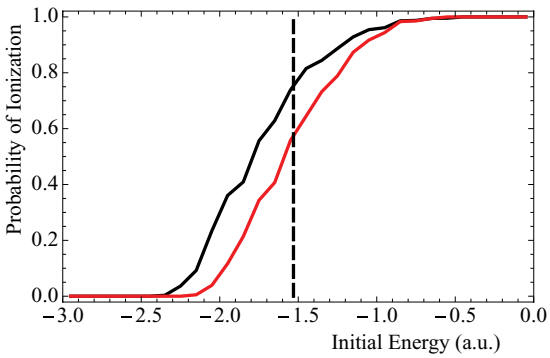

FIG. 7. (Color online) Ionization probability vs initial energy for the two-dimensional system, with $a = 0.01$, for intervals of 2.75 (lower curve) and 4.75 cycles (upper curve). The vertical dashed line shows the energy of the maximally suppressed barrier.

for an ionized electron with low drift velocity to reattach when the laser field turns off, which is a process sometimes referred to as frustrated ionization [20].

Also, we note that the smoother curves at the highest energies in Fig. 6 arise because the dynamics of electrons that begin with higher energy are dominated by the laser field (with different results in 1D depending on the sign of the initial position). In analogy with the results of Mauger *et al.* [13], the 1D case shows an energy region in which escape is possible, but not assured. This "sticky" region extends to noticeably higher energies in the 2D case, indeed well above the threshold marked by the vertical bar.

It is natural to expect that if a longer time interval was considered, additional electrons might ionize. Thus we have repeated the analysis through $t = 4.75$ cycles and calculated the fraction of trajectories that ionize. Results for $t = 2.75$ and 4.75 cycles are superposed in Fig. 7 and confirm the expectation.

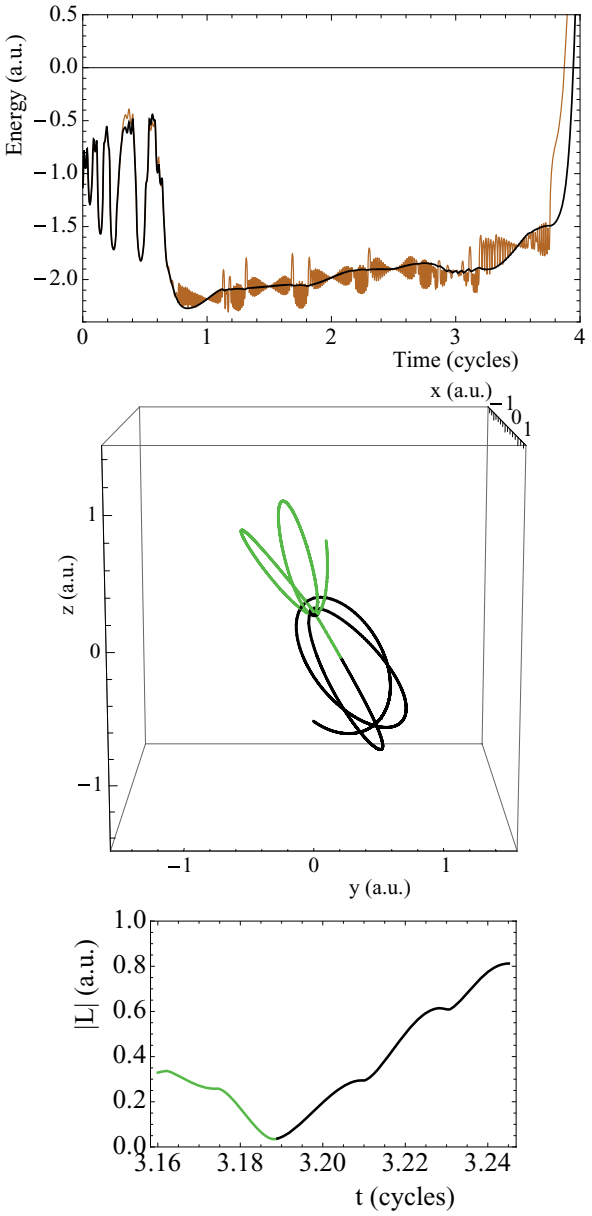

FIG. 8. (Color online) Top plot shows energy vs time for one sequential-ionization electron from our 3D ensemble, for $a = 0.01$ and $I = 3 \times 10^{15}$ W/cm^2 over the interval $0.0 < t < 4.0$ cycles. As in Fig. 2, the highly oscillatory (brown) curve neglects the laser interaction energy. The middle plot shows the electron position for $3.16 < t < 3.24$ cycles. The curve changes from green to black (light to dark) at $t = 3.19$ cycles. The bottom plot shows the magnitude of angular momentum, $|L|$, for the same time interval, and with color change at the same time. At about this time, the electron jumps from orbiting primarily on the $z > 0$ side of the nucleus to oscillating primarily on the $z < 0$ side, and the laser does considerable positive work.

IV. ENERGY ABSORPTION IN THREE DIMENSIONS

We return now to examining sequential ionization in our 3D ensembles that led to Fig. 1. In Fig. 8, we examine one specific trajectory for intensity 3×10^{15} W/cm^2, which is one of the lowest intensities at which sequential double ionizations occur. The upper plot shows energy on the time interval from $t = 0.0$ to 4.0 cycles, and the middle plot shows the spatial trajectory from 3.16 to 3.24 cycles.

The upper plot shows the various stages in the double-ionization process. Initially the two electrons jostle each other and there is considerable energy fluctuation for an individual electron. At first ionization, the remaining electron drops low in the well. There is no recollision. Instead, the electron gains energy from the field—especially in the time interval from 3 to 4 cycles—and escapes. The plots indicate that at about 3.2 cycles, slightly before the laser maximum, the electron jumps from an orbit that favors $z > 0$ to an orbit that favors $z < 0$. The laser force is given by $-zE_0 f(t)\sin\omega t$, and the

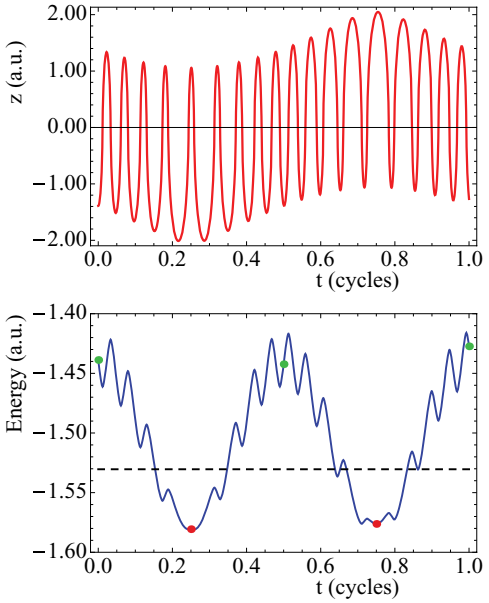

FIG. 9. (Color online) Top panel: Position vs time for an electron in 1D; $I = 3 \times 10^{15}$ W/cm^2 with $\lambda = 800$ nm and $a = 0.01$. Bottom panel: Energy vs time, with the laser interaction included. The energy of the maximally suppressed barrier is shown as a dashed (black) line. Dots show energies at the time of laser zeros (upper dots) and maxima (lower dots).

electron's jump takes it toward the side of the nucleus toward which the laser force is pushing, i.e., toward the downhill side of the potential-energy curve. Then, as the laser force diminishes over the quarter cycle from 3.25 to 3.5 cycles, the electron gains energy as the $z < 0$ side of the curve rises. From 3.5 until about 3.75 cycles, it stays on the $z < 0$ side, where the potential-energy curve is continuing to rise. (The highly oscillatory curve is below the smoother curve whenever the electron is on the "uphill" side of the nucleus, and above the smoother curve whenever the electron is on the "downhill" side.) Then, when the field is strong, the electron jumps to the downhill side of the potential curve and escapes over the suppressed barrier.

This confirms that the energy-absorption mechanism, which we discussed for our 2D one-electron system, is also present in our 3D classical ensemble model. A check of multiple trajectories reveals that this mechanism is indeed responsible for the early onset of the sequential ionization when the nuclear force is minimally softened.

V. LACK OF ENERGY ABSORPTION IN 1D

We round out this paper by looking at the one-dimensional model that we used for the top row of Fig. 6. An example of a 1D case is depicted in Fig. 9 for $a = 0.01$. The top plot shows position z vs time over a single cycle, and the bottom plot shows electron energy vs time (including the laser interaction energy). Snapshots of the nuclear potential-energy well at specific times are shown in Fig. 10. For this one-dimensional case, the electron cannot backscatter off the nucleus, but

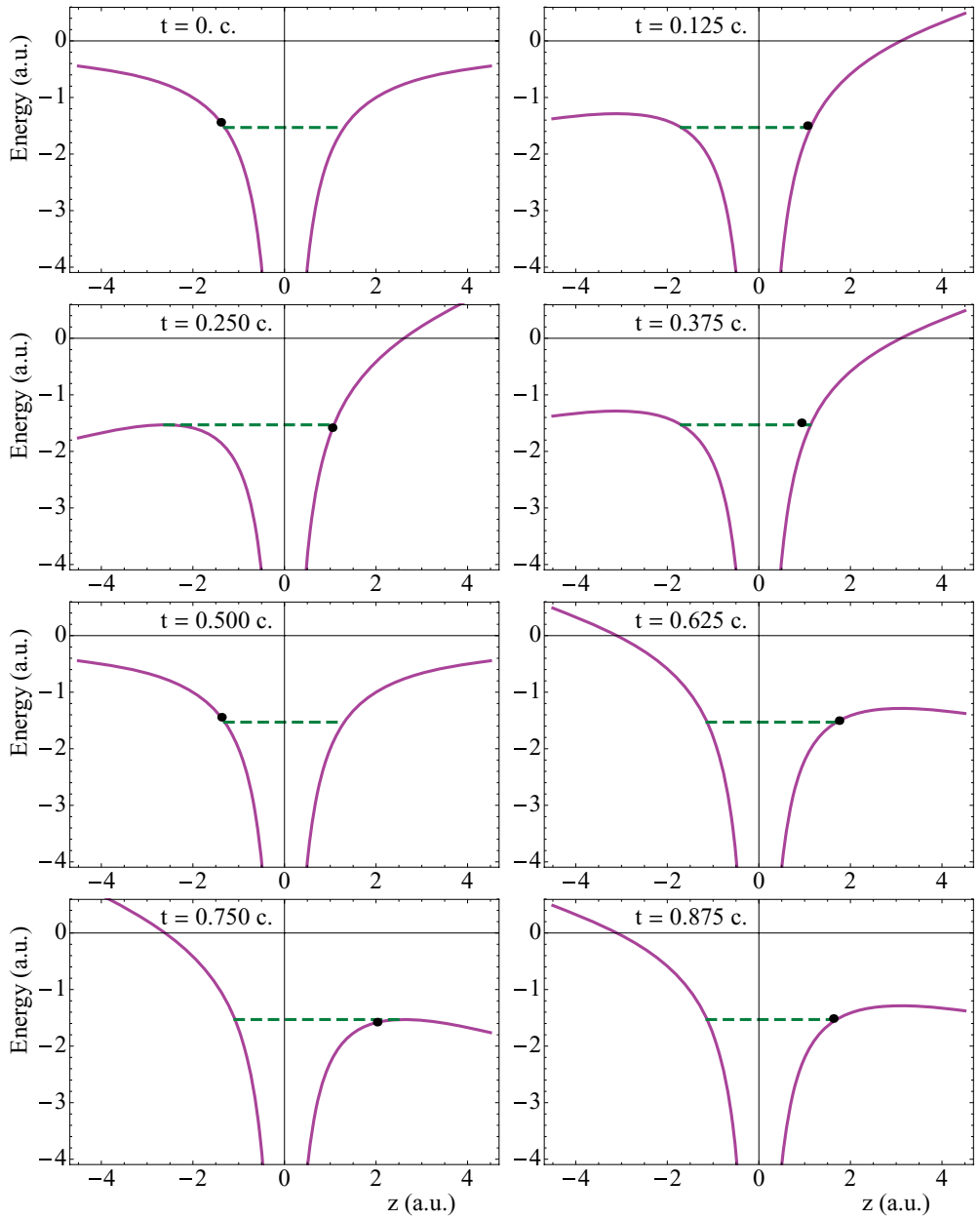

FIG. 10. (Color online) Effective energy plots of the electron of Fig. 9 over 1 laser cycle in intervals of 0.125 cycles. The horizontal line shows the energy of the maximally suppressed barrier. The electron never escapes.

always overshoots (regardless of the value of the softening parameter). This overshoot is clearly evident in the plot of z vs t. Nonetheless, from $t = 0$ to 0.5 cycles, there is a slight preference for $z < 0$, and from $t = 0.5$ to 1.0 cycles, there is a slight preference for $z > 0$. This preference is toward the direction of the laser force and the downhill side of the potential-energy curve (Fig. 10).

The energy curve (Fig. 9), which is on a finer energy (vertical) scale than our other energy plots, shows rapid oscillations superposed on slower, larger oscillations. The rapid energy oscillations occur as the electron moves from one side of the nucleus to the other. The electron gains energy when it is on the side of the nucleus where the field is increasing (i.e., the potential curve is rising) and loses energy when on the other side. The energy includes the laser interaction energy, so these oscillations are different from the large rapid oscillations that arose in Figs. 2 and 3. The visibility of these fluctuations is, to a large extent, due to the fine energy resolution we are using, as well as the distance the electron overshoots the nucleus each orbit—a close examination of the smooth curve in the top plot of Fig. 3 shows small oscillations as well.

The slower oscillations visible in Fig. 9 occur at twice the laser frequency, with peak energy at about the time of each laser zero (indicated by green, light dots) and minimum energy at about the laser maxima (red, dark dots). These slower oscillations occur because the electron spends more time on the downhill side of the well than the uphill side. Consequently, after each laser zero, the electron shows an overall energy loss as the downhill side drops, then an increase as the curve rises again. The dashed line across the graph shows the barrier suppression energy. Over most of the cycle, the electron actually has energy above the barrier, but the electron energy is near its minimum when the barrier is maximally suppressed and the electron remains trapped. This example illustrates why Fig. 6 indicated the need for starting the energy above the barrier. (We recall that the starting energy was defined at a zero of the laser field, not at a laser maximum.)

VI. CONCLUDING COMMENTS

We have noted that in three-dimensional classical ensembles, the ability of a single electron in a nuclear potential-energy well to absorb energy from an oscillating laser field depends critically on the steepness of the well close to the nucleus. If the electron is in a low-angular momentum orbit that takes it close to the nucleus, then a large force from the nucleus can backscatter the electron; thus its orbit can be primarily on one side of the nucleus. If this orbit lies primarily on the side of the nucleus for which the potential energy from the interaction with the laser is increasing, then the electron can "ride" the increasing potential energy toward greater energy. If the orbit was always on the same side of the nucleus, such an increase would be balanced by a decrease during the subsequent half cycle. However, we found that the laser force can help the electron to jump from an orbit that favors one side of the nucleus to an orbit that favors the opposite side. If this jump occurs at about the time of the peak laser field, then the electron can ride the increasing potential-energy curve over successive half cycles, gain significant energy, and escape the well.

In one-dimensional systems, the electron always overshoots the nucleus and the electron can remain trapped in the well. Similarly, in two or three dimensions, if the nuclear force has been softened, then the electron may simply overshoot the core area, and consequently be trapped in the well.

We have not sought here to apply these ideas to specific physical systems, but instead have analyzed and emphasized what can happen within classical models. We hope that these ideas and insights will be helpful to other researchers who employ classical models to understand complex atomic or molecular systems in external fields.

ACKNOWLEDGMENTS

This material is based upon work supported by the National Science Foundation under Grant No. 0969984 to Calvin College. Some computations in this paper were performed on dahl.calvin.edu, a Beowulf cluster built with support from the National Science Foundation's Major Research Instrumentation and Cyber Infrastructure programs, Grant No. OCI-0722819. We acknowledge the contributions of T. L. Atallah.

[1] For reviews of NSDI, see R. Dörner *et al.*, Adv. Atom. Molec. Opt. Phys. **48**, 1 (2002); A. Becker, R. Dörner, and R. Moshammer, J. Phys. B **38**, S753 (2005); A. Becker and F. H. M. Faisal, *ibid.* **38**, R1 (2005); W. Becker and H. Rottke, Contemp. Phys. **49**, 199 (2008).

[2] For a review article regarding the use of the many-body S-matrix theory in NSDI, see A. Becker and F. H. M. Faisal, J. Phys. B **38**, R1 (2005).

[3] K. J. Schafer, B. Yang, L.F. DiMauro, and K.C. Kulander, Phys. Rev. Lett. **70**, 1599 (1993); P. B. Corkum, *ibid.* **71**, 1994 (1993).

[4] J. S. Parker, B. J. S. Doherty, K. T. Taylor, K. D. Schultz, C. I. Blaga, and L. F. DiMauro, J. Phys. B **36**, L393 (2003); Phys. Rev. Lett. **96**, 133001 (2006).

[5] D. G. Lappas *et al.*, J. Phys. B **29**, L619 (1996); D. Bauer, Phys. Rev. A **56**, 3028 (1997); W.-C. Liu, J. H. Eberly, S. L. Haan, and R. Grobe, Phys. Rev. Lett. **83**, 520 (1999).

[6] J. Javanainen, J. H. Eberly, and Q. Su, Phys. Rev. A **38**, 3430 (1988); Q. Su and J. H. Eberly, *ibid.* **44**, 5997 (1991); R. Grobe and J. H. Eberly, Phys. Rev. Lett. **68**, 2905 (1992).

[7] S. L. Haan, P. S. Wheeler, R. Panfili, and J. H. Eberly, Phys. Rev. A **66**, 061402(R) (2002).

[8] R. Panfili, J. H. Eberly, and S. Haan, Opt. Express **8**, 431 (2001).

[9] S. L. Haan, L. Breen, A. Karim, and J. H. Eberly, Phys. Rev. Lett. **97**, 103008 (2006); Opt. Express **15**, 767 (2007).

[10] S. L. Haan, Z. S. Smith, K. N. Shomsky, and P. W. Plantinga, J. Phys. B **42**, 134009 (2009).

[11] P. J. Ho and J. H. Eberly, Phys. Rev. Lett. **97**, 083001 (2006).
[12] See, for example, Q. Liao and P. Lu, Opt. Express **17**, 15550 (2009).
[13] F. Mauger, C. Chandre, and T. Uzer, Phys. Rev. Lett. **102**, 173002 (2009); Phys. Rev. A **81**, 063425 (2010).
[14] T. Brabec, M. Y. Ivanov, and P. B. Corkum, Phys. Rev. A **54**, R2551 (1996).
[15] S. L. Haan and Z. S. Smith, Phys. Rev. A **76**, 053412 (2007).
[16] We previously presented the curve for $a = 0.4$ in S. L. Haan, Z. S. Smith, K. N. Shomsky, P. W. Plantinga, and T. L. Atallah, Phys. Rev. A **81**, 023409 (2010).
[17] We define the ionization to be sequential if the first electron to ionize does not return to within $r = 5$ of the nucleus or if energy transfer to the second electron is less than 0.1 a.u.
[18] Effective energy diagrams were introduced in R. Panfili, S. L. Haan, and J. H. Eberly, Phys. Rev. Lett. **89**, 113001 (2002), and adapted for 3D in Ref. [9], part b.
[19] Y. Zhou, Q. Liao, and P. Lu, Phys. Rev. A **80**, 023412 (2009).
[20] T. Nubbemeyer, K. Gorling, A. Saenz, U. Eichmann, and W. Sandner, Phys. Rev. Lett. **101**, 233001 (2008); K. N. Shomsky, Z. S. Smith, and S. L. Haan, Phys. Rev. A **79**, 061402(R) (2009).